

# Quantum Mechanical Carrier Transport and Nano-scale MOS Modeling

Zhiping Yu and Dawei Zhang  
Institute of Microelectronics  
Tsinghua University, Beijing, China  
yuzhip@tsinghua.edu.cn

2nd Hiroshima Int'l Workshop  
Jan. 30, 2004



## Outline

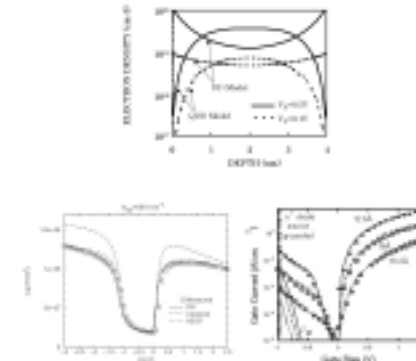
- Introduction
- Schrödinger Equation and Wigner Function
- Macroscopic Modeling Approach
  - Quantum Hydrodynamic (QHD)
  - Density Gradient (DG)
  - Effective Potential (EP)
- Microscopic Modeling Approach
  - QTBM (Quantum Transmitting Boundary Method)
  - QDAME (Quan. Dev. Ana. by Modal Evaluation)
  - NEGF (Non-equilibrium Green's Function)
- Numerical Model for 3D FinFETs
- Ballistic MOS Model (BMM)



## Introduction

Manifestation of quantum mechanical effects on MOS characteristics:

- Increasing effective gate oxide thickness with consequence of
  - Smaller gate capacitance
  - Larger threshold voltage
- Tunneling current
  - through gate oxide
  - through barrier between S/D along the channel
- Ballistic transport
- Subthreshold slope



Modeling approaches:

- Macroscopic: particle (solve Shockley semiconductor eqs.)
  - Quantum hydrodynamic model (QHD)
  - Density gradient drift-diffusion (QDD)
  - Effective potential approach (EP)
- Microscopic: wavefunction (solve Schrödinger eq.)
  - Quantum transmitting boundary method (QTBM)
  - Modified QTBM – QDAME
  - Green's function approach – NEGF
- Compact circuit model
  - Changing threshold voltage
  - Model ballistic transport (transmission theory)



5/48



## Schrödinger Equation and Wigner Function

- Schrödinger Equation

$$\left[ -\frac{\hbar^2}{2m^*} \nabla^2 + U(\mathbf{r}) \right] \Psi(\mathbf{r}) = E\Psi(\mathbf{r}) \quad (1)$$

- Wigner Function

$$f_W(\mathbf{r}, \mathbf{p}) = \frac{1}{(\pi\hbar)^3} \int \Psi^*(\mathbf{r} + \mathbf{r}') \Psi(\mathbf{r} - \mathbf{r}') e^{2i\mathbf{p}\cdot\mathbf{r}'/\hbar} d\mathbf{r}' \quad (2)$$

Momentum-shifted Wigner function

$$f_W^{(2)}(\mathbf{x}, \mathbf{p}) = \mathcal{A} \frac{e^{-\beta E}}{(2\pi\hbar)^3} \left\{ 1 + \hbar^2 \left[ -\frac{\beta^2}{8m^*} \nabla^2 U + \frac{\beta^3}{24m^*} (\nabla U \cdot \nabla U) + \frac{\beta^3}{24m^*} (\mathbf{p}' \cdot \nabla)^2 U \right] \right\} \quad (3)$$

where  $\mathbf{p}' = \mathbf{p} - m^*\mathbf{u}$  with  $\mathbf{u}$ , the macroscopic fluid (or drift) velocity, and  $E = p^2/2m^* + U$ .



6/48



- Wigner-Boltzmann Equation

$$\frac{\partial f_W}{\partial t} + \frac{\mathbf{p} \cdot \nabla f_W}{m^*} - \frac{2}{\hbar} \sin\left(\frac{\hbar}{2} \nabla U \cdot \nabla_{\mathbf{p}}\right) U(\mathbf{r}) f_W(\mathbf{r}, \mathbf{p}) = 0 \quad (4)$$

Or use the integral form by defining the nonlocal potential energy

$$\hat{U}(\mathbf{r}, \mathbf{p}) = 2 \int \sin\left(\frac{\mathbf{p} \cdot \mathbf{y}}{\hbar}\right) [U(\mathbf{r} + \mathbf{y}/2) - U(\mathbf{r} - \mathbf{y}/2)] d\mathbf{y} \quad (5)$$

The Wigner-Boltzmann eq. then takes form of

$$\frac{\partial f_W}{\partial t} + \frac{\mathbf{p} \cdot \nabla f_W}{m^*} - \frac{2}{\hbar} \int \frac{1}{2\pi\hbar} \hat{U}(\mathbf{r}, \mathbf{p} - \mathbf{p}') f_W(\mathbf{r}, \mathbf{p}') d\mathbf{p}' = 0 \quad (6)$$



7/48



## Moment Approach – QHD

- Retaining terms up to  $\hbar^2$  in the series expansion of Eq. (4) and take first three moments in  $\mathbf{p}$ -space: 1,  $\mathbf{p}$ ,  $\mathbf{p} \cdot \mathbf{p}/2m^*$ .
- Quantum Hydrodynamic Equations

$$\frac{\partial n}{\partial t} + \frac{1}{m^*} \nabla \cdot \mathbf{\Pi} = 0 \quad (7)$$

$$\frac{\partial}{\partial t} \Pi_i + \nabla \cdot (\mathbf{u} \Pi_i) - \sum_{j=1}^3 \frac{\partial P_{ji}}{\partial x_j} = -n \frac{\partial U}{\partial x_i} - \frac{1}{\tau_p} \Pi_i, \quad i = 1, 2, 3 \quad (8)$$

$$\frac{\partial W}{\partial t} + \nabla \cdot (\mathbf{u} W - \hat{P} \mathbf{u} + \mathbf{q}) = -\frac{1}{m^*} \mathbf{\Pi} \cdot \nabla U - \frac{W - W_0}{\tau_w} \quad (9)$$

for variables  $n$ ,  $\mathbf{u}$ , and energy density  $W$ , where  $\mathbf{\Pi} = nm^*\mathbf{u}$  is the momentum density and  $\hat{P}$  the stress tensor.

- Quantum corrections

The gradient of carrier density is a manifestation of non-locality, which is the essence of quantum mechanics.



8/48



– Stress tensor

$$\hat{P} = -nTI + \frac{\hbar^2 n}{12m^*}(\nabla\nabla) \ln n \quad (10)$$

– Energy density

$$W = \frac{3}{2}nT + \frac{1}{2}m^*nu^2 - \frac{\hbar^2 n}{24m^*}\nabla^2 \ln n \quad (11)$$

– A compact form

$$\nabla \cdot (\nabla \ln n) = -\frac{1}{n^2}\nabla n \cdot \nabla n + \frac{1}{n}\nabla^2 n \quad (12)$$

$$2\frac{\nabla^2 \sqrt{n}}{\sqrt{n}} = -\frac{1}{2n^2}\nabla n \cdot \nabla n + \frac{1}{n}\nabla^2 n \quad (13)$$



9/48



## Density Gradient (DG) Drift-Diffusion Model

$$V_n = V + Q_n \quad (14)$$

$$V_p = V - Q_p \quad (15)$$

where quantum potential

$$Q_n = 2b_n \frac{\nabla^2 \sqrt{n}}{\sqrt{n}}, \quad b_n = \frac{\hbar^2}{12qm_n^*} \quad (16)$$

$$Q_p = 2b_p \frac{\nabla^2 \sqrt{p}}{\sqrt{p}}, \quad b_p = \frac{\hbar^2}{12qm_p^*} \quad (17)$$

$V_n$  and  $V_p$  are used in the place of  $V$  for conventional DD formulation, e.g.,

$$n = n_i e^{(V_n - \phi_n)/V_T} \quad (18)$$

$$p = n_i e^{(\phi_p - V_p)/V_T} \quad (19)$$



10/48



The carrier fluxes are expressed as

$$\mathbf{F}_n = -D_n \nabla n + \mu_n n \nabla V_n \quad (20)$$

$$\mathbf{F}_p = -D_p \nabla p - \mu_p p \nabla V_p \quad (21)$$

Solving Shockley semiconductor equations for  $n$ ,  $p$ , and  $V$

$$\nabla \cdot (\epsilon \nabla V) = -q(p - n + N_D^+ - N_A^-) \quad (22)$$

$$\nabla \cdot \mathbf{F}_n + r = 0 \quad (23)$$

$$\nabla \cdot \mathbf{F}_p + r = 0 \quad (24)$$

### Solution approaches

(main challenge: the robustness of the method)

- Trade number of variables to the order of derivative
- Five variables:  $V$ ,  $S_n = \sqrt{n}$ ,  $S_p = \sqrt{p}$ ,  $\phi_n$ , and  $\phi_p$ .



11/48



Equation set:

$$\nabla \cdot (\epsilon \nabla V) + q(p - n + N_D^+ - N_A^-) = 0 \quad (25)$$

$$\nabla \cdot (b_n \nabla S_n) + \frac{S_n}{2} \left( V - \frac{k_B T}{q} \ln \frac{n}{n_i} - \phi_n \right) = 0 \quad (26)$$

$$\nabla \cdot (b_p \nabla S_p) - \frac{S_p}{2} \left( V + \frac{k_B T}{q} \ln \frac{p}{n_i} - \phi_p \right) = 0 \quad (27)$$

$$\nabla \cdot (\mu_n n \nabla \phi_n) + \frac{\partial n}{\partial t} + r = 0 \quad (28)$$

$$\nabla \cdot (\mu_p p \nabla \phi_p) - \frac{\partial p}{\partial t} - r = 0 \quad (29)$$

The disadvantage of this scheme is when  $b \rightarrow 0$ , the Helmholtz equations, Eqs. (26-27) becomes singular. The convergence behavior is poor, often needs to keep the bias step small to prevent negative  $S_n(\sqrt{n})$  and  $S_p(\sqrt{p})$ .



12/48



Results

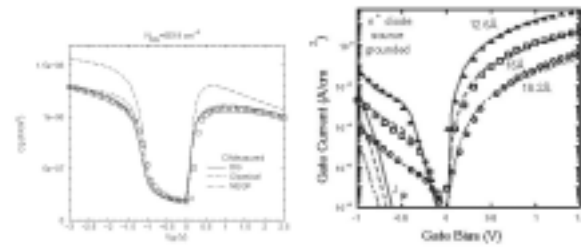


Figure 1: Measured and simulated C-V for  $t_{ox} = 2.1$  nm and tunneling through MOS gate structure using DG.

13/48

⏪ ⏩ ⏴ ⏵ ⏶ ⏷ ⏸ ⏹ ⏺ ⏻ ⏼ ⏽ ⏾ ⏿

- Use variables  $V, u_n, u_p, \phi_n,$  and  $\phi_p$  (Prof. Shinji Odanaka of Osaka Uni.) where

$$u_n = \frac{V_n - \phi_n}{2}, \quad u_p = \frac{\phi_p - V_p}{2} \quad (30)$$

The advantage with variable  $u$ 's is that the carrier concentration is guaranteed to be positive, e.g.,

$$S_n = \sqrt{n} = \sqrt{n_i} e^{u_n/V_T} \quad (31)$$

The eq. for  $u_n$  is

$$-b_n \nabla \cdot (S_n \nabla u_n) + S_n u_n = \frac{S_n}{2} (V - \phi_n) \quad (32)$$

This eq. is of Sturm-Liouville type of problem for  $u_n$  given  $S_n, V,$  and  $\phi_n$ .

14/48

⏪ ⏩ ⏴ ⏵ ⏶ ⏷ ⏸ ⏹ ⏺ ⏻ ⏼ ⏽ ⏾ ⏿

Results:

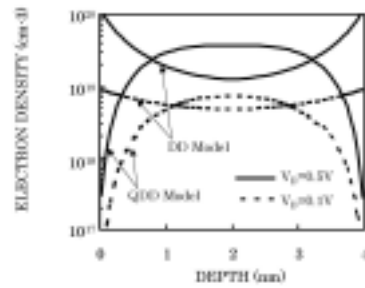


Figure 2: Carrier distribution in double gate MOSFET ( $t_{si} = 5$  nm,  $t_{ox} = 1.5$  nm,  $L_g = 25$  nm).

The advantage: robustness – The drain bias can jump to 0.5V in one step.

15/48

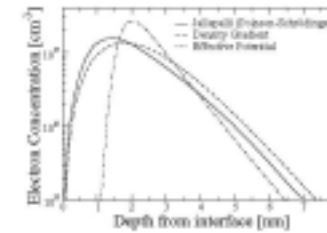
⏪ ⏩ ⏴ ⏵ ⏶ ⏷ ⏸ ⏹ ⏺ ⏻ ⏼ ⏽ ⏾ ⏿

## Effective Potential (EP) Model

- Considering electron wavepacket as finite in size

$$V_{eff} = \int V_{cl}(\mathbf{x} + \mathbf{y}) G(\mathbf{y}, a_0) d\mathbf{y} \quad (33)$$

- Comparison between DG and EP models



16/48

⏪ ⏩ ⏴ ⏵ ⏶ ⏷ ⏸ ⏹ ⏺ ⏻ ⏼ ⏽ ⏾ ⏿

- Similarity with DG

$$V_{\text{eff}}(x) = \frac{1}{\sqrt{2\pi a_0}} \int V(x + \xi) e^{-\xi^2/2a_0^2} d\xi$$

$$\approx V(x) - \frac{2a_0^2}{\beta} \frac{\partial^2 \ln \sqrt{n/n_0}}{\partial x^2} + \dots \quad (34)$$

Poor accuracy of EP may be due to the missing of another term with the same order as  $\hbar^2$ .

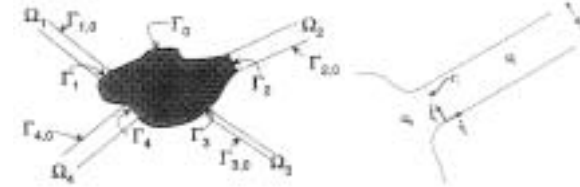


17/48



## Microscopic QM Transport

- Quantum Transmitting Boundary Model (QTBM)



Find  $\Psi_0(\mathbf{r}) \in C^2(\Omega_0)$ , knowing the form of  $\Psi_i(\xi_i, \eta_i) \in C^2(\Omega_i)$ ,  $i = 1, \dots, n$ . The boundary condition for  $\Psi_0$  in  $\Omega_0$  is

$$\Psi_0 = 0 \text{ on } \Gamma_0 = \partial\Omega_0 - \sum_{i=1}^n \Gamma_i \quad (35)$$

$$\Psi_0 = \Psi_i \text{ on } \Gamma_i \quad (36)$$

$$\nabla \Psi_0 \cdot \mathbf{n}_{\Gamma_i} = \nabla \Psi_i \cdot \mathbf{n}_{\Gamma_i} \text{ on } \Gamma_i \quad (37)$$



18/48



General solution procedure:

- The solution in the lead  $i$  has the form of

$$\psi_i(\xi_i, \eta_i) = \sum_{m=1}^{N_i} \left[ a_m^i \chi_m^i(\xi_i) e^{-jk_m^i \eta_i} + b_m^i \chi_m^i(\xi_i) e^{jk_m^i \eta_i} \right]$$

$$+ \sum_{m=N_i+1}^{\infty} b_m^i \chi_m^i(\xi_i) e^{-jk_m^i \eta_i} \quad (38)$$

- Eliminating the explicit dependence on  $\Psi_i$ , a mixed BC for  $\Psi_0$  on  $\Gamma_i$  is obtained as

$$\nabla \Psi_0 \cdot \mathbf{n}_{\Gamma_i} |_{\xi_i} = \sum_{i=1}^{N_i} ik_m^i \chi_m^i(\xi_i) \left( -2a_m^i + \int_{\Gamma_i} \chi_m^i(\Gamma_i) \Psi_0(\Gamma_i) d\Gamma_i \right)$$

$$- \sum_{m=N_i+1}^{\infty} k_m^i \chi_m^i(\xi_i) \int_{\Gamma_i} \chi_m^i(\Gamma_i) \Psi_0(\Gamma_i) d\Gamma_i \quad (39)$$



19/48



- Quantum Device Analysis by Mode Evaluation (QDAME)

Based on QTBM and has the following features:

- Able of evaluating  $I$ - $V$  characteristics
- Discretely sample a device's density of states using standing wave boundary conditions, decomposing the standing waves into traveling waves injected from the contacts to assign occupancies.

Solution procedure:

1. Find standing wavefunctions by imposing (at  $\Gamma_i$ )

$$\text{sine : } \Psi_n^{(s)} = 0 \implies E_n^{(s)}$$

$$\text{cosine : } \nabla \Psi_n^{(c)} \cdot \mathbf{n}_{\Gamma_i} = 0 \implies E_n^{(c)}$$



20/48



2. Decompose the normal mode into traveling components

$$\Psi_n^{(s,c)}(\mathbf{r}) = \sum_i \Phi_{n,i}^{(s,c)}(\mathbf{r}) \quad (40)$$

3. Given the normal mode energy and the injection coefficients, the traveling components are computed using a modified version of the QTBM.

4. The electron density  $n(\mathbf{r})$  is the sum of electron densities from the sine sampling  $n^{(s)}(\mathbf{r})$  and cosine sampling  $n^{(c)}(\mathbf{r})$ , found by summing over all traveling eigen-component densities multiplied by a thermal occupation factor

$$n(\mathbf{r}) = \sum_{s,c} n^{s,c}(\mathbf{r}) = \sum_{s,c} \left\{ \sum_{n,i} |\Phi_{n,i}^{s,c}(\mathbf{r})|^2 \sum_p c_{p,n,i}^{s,c} \rho(k_D^i, T, E_n^{s,c}) \right\} \quad (41)$$

where the thermal occupancy factor is the sum of occupancy factor  $\rho(k_D^i, T, E_n^{s,c})$  and coefficients  $c_{p,n,i}^{s,c}$  representing the frac-



tional weight of each mode  $p$  in lead  $i$  making up the traveling eigen-component.

Drifted Fermi-Dirac occupancy factor

$$\rho(k_{Di}, T, E) = \left( \frac{8m_z^i k_B T}{h^2} \right)^{1/2} \times F^{-1/2} \left( \frac{E_{Fi} - E - \frac{\hbar^2}{2m_z^i} k_D^i (k_D^i - 2k_\eta^{p,i})}{k_B T} \right) \quad (42)$$

where the drift momentum  $\hbar k_D^i$  in lead  $i$  is found from the current continuity requirement between lead and device.



### • Non-equilibrium Green's Function (NEGF)

NEGF provides a microscopic theory for quantum transport including dissipative interaction.

Green's function,  $G^R(\mathbf{r}, \mathbf{r}')$ , is obtained from solving Schrödinger equation with boundary conditions

$$[E - H_d]G^R(\mathbf{r}, \mathbf{r}') - \int \Sigma^R(\mathbf{r}, \mathbf{r}_1)G^R(\mathbf{r}_1, \mathbf{r}')d\mathbf{r}_1 = \delta(\mathbf{r} - \mathbf{r}') \quad (43)$$

which can be viewed as the wavefunction at the point  $\mathbf{r}$  due to a unit excitation at  $\mathbf{r}'$ .

Without the source term, the above Green's function becomes the Schrödinger-like equation with boundary condition built-in it:

$$E\Psi(\mathbf{r}) = H_d\Psi(\mathbf{r}) + \int \Sigma^R(\mathbf{r}, \mathbf{r}_1)\Psi(\mathbf{r}_1)d\mathbf{r}_1 \quad (44)$$

which describes the dynamics of an electron inside the device region.



Matrix form of Green's function

$$G^R = [EI - H_d - \Sigma^R]^{-1} \quad (45)$$

The use of Green's functions

– DOS:  $G^R$  and its conjugate transpose  $G^A = [G^R]^\dagger$  represent the density of states in the energy space.

$$N(E) = \frac{1}{2\pi} \text{Tr} \{i[G^R(E) - G^A(E)]\} \quad (46)$$

Or the position-dependent density of states

$$\rho(\mathbf{r}, E) = -\frac{1}{\pi} \text{Im} [G^R(\mathbf{r}, \mathbf{r}; E)] \quad (47)$$



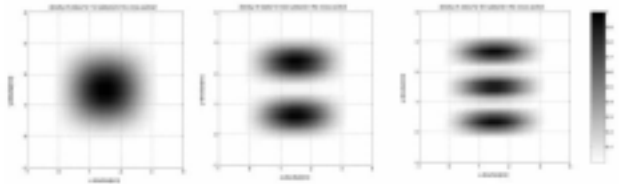


Figure 3: DOS on the cross-section (3nm×3nm) of a FinFET

25/48

– **Carrier concentration:** can be expressed using the so-called correlation function  $G^n$ :

$$G^n(\mathbf{r}, \mathbf{r}') = \int \int G^R(\mathbf{r}, \mathbf{r}_1) \Sigma^{\text{in}}(\mathbf{r}_1, \mathbf{r}'_1) [G^R(\mathbf{r}', \mathbf{r}'_1)]^* d\mathbf{r}_1 d\mathbf{r}'_1 \quad (48)$$

where  $\Sigma^{\text{in}}$  is the inscattering function related to  $\Sigma^R$  and the quasi-Fermi level on the contact as in

$$\Sigma_p^{\text{in}}(\mathbf{r}, \mathbf{r}'; E) = f_p(E, \mu_p) \Gamma_p(\mathbf{r}, \mathbf{r}'; E) \quad (49)$$

where  $p$  represents the contact (or the lead) and  $\mu_p$  is the quasi-Fermi level for that contact and  $\Gamma = i [\Sigma^R - \{\Sigma^R\}^\dagger]$ .

$$\Sigma^R = \Sigma_\varphi^R + \sum_p \Sigma_p^R \quad (50)$$

$$\Sigma_p^R(i, j; E) = -\frac{\hbar^2}{2m^* a^2} \sum_{m \in p} \chi_m(p_i) e^{ik_m a} \chi_m(p_j) \quad (51)$$

26/48

The carrier concentration is

$$n(\mathbf{r}) = 2 \int \frac{1}{2\pi} G^n(\mathbf{r}, \mathbf{r}; E) dE \quad (52)$$

where the pre-factor 2 is for the spin degeneration.

– **Current density:** The current density inside the device is

$$\mathbf{j}(\mathbf{r}; E) = -\frac{iq\hbar}{2m^*} [(\nabla - \nabla') G^n(\mathbf{r}, \mathbf{r}'; E)]_{\mathbf{r}=\mathbf{r}'} \quad (53)$$

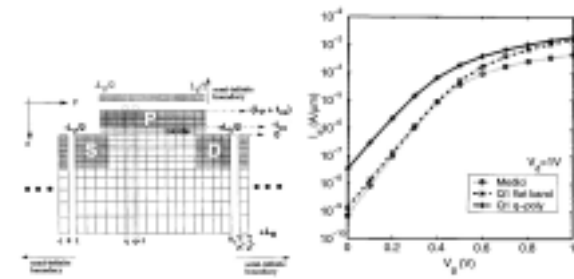
where the gradient operator  $\nabla'$  means that it only acts on  $\mathbf{r}'$ . The terminal current per unit energy is

$$i(E) = \int \mathbf{j}(\mathbf{r}, E) \cdot d\mathbf{S} \quad (54)$$

27/48

## 2D MOS Simulation using NEGF

– NASA's simulation of 2D MOSFET with NEGF, including a self-consistent treatment of 2D gate oxide tunneling.



28/48

Comparison with DG:

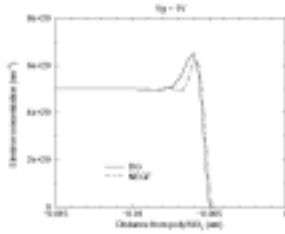


Figure 4: Electron distribution in the poly-gate region using DG and NEGF for MIT *wtm* 25 ( $L_{ch} = 25$  nm).

  
29/48

⏪ ⏩ ⏴ ⏵ ⏮ ⏭ ⏯ ⏰

## Quasi-3D Numerical Model for FinFETs

- Simulation method:
  - Schrödinger eq. solver on 2D cross-section
  - NEGF along the channel
  - 3D Poisson's solver
- Device structure

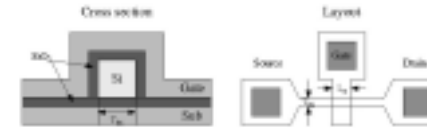


Figure 5: FinFET structure and layout

  
30/48

⏪ ⏩ ⏴ ⏵ ⏮ ⏭ ⏯ ⏰

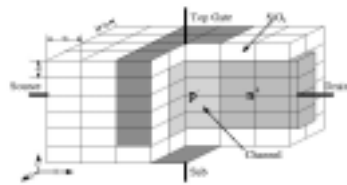


Figure 6: Simulation region and mesh

- Simulation details
  - Separation of variables and WKB theory on  $x$ -direction

$$\Psi(x, y, z) = X(x)\varphi(y, z) = e^{ik_x x} \varphi(y, z) \quad (55)$$

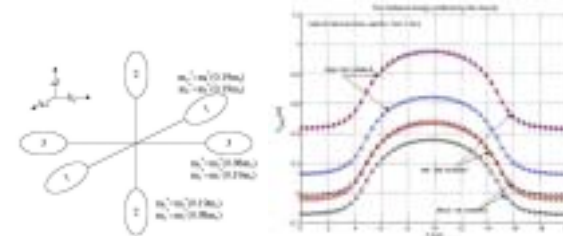
  
31/48

⏪ ⏩ ⏴ ⏵ ⏮ ⏭ ⏯ ⏰

– 2D Schrödinger eq. on  $y$ - $z$  cross-section

$$\left( -\frac{\hbar^2}{2m_y^*} \frac{\partial^2}{\partial y^2} - \frac{\hbar^2}{2m_z^*} \frac{\partial^2}{\partial z^2} \right) \Psi_x^i(y, z) - qV_x(y, z) \Psi_x^i(y, z) = E_{i,x}^i \Psi_x^i(y, z) \quad (56)$$

– Bounded states affected by different effective mass

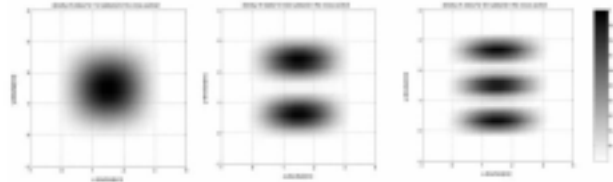


  
32/48

⏪ ⏩ ⏴ ⏵ ⏮ ⏭ ⏯ ⏰



- 2D density of states (DOS)



33/48

- NEGF solution of 1D Schrödinger eq. with open BC for density matrix in energy representation

$$H X(x) = \left[ -\frac{\hbar^2}{2m_x^*} \frac{\partial^2}{\partial x^2} + E_t(x) \right] X(x) = E X(x) \quad (57)$$

$$G(E) = [EI - H - \Sigma(E)]^{-1} \quad (58)$$



where the self-energy matrix

$$\Sigma = \begin{bmatrix} \Sigma_{\text{source}} & 0 & \cdots & 0 & 0 \\ 0 & \Sigma_s(1) & \cdots & 0 & 0 \\ \vdots & \vdots & \ddots & \vdots & \vdots \\ 0 & 0 & \cdots & \Sigma_s(n) & 0 \\ 0 & 0 & \cdots & 0 & \Sigma_{\text{drain}} \end{bmatrix} \quad (59)$$

For ballistic transport (neglecting scattering),  $\Sigma_s(i) = 0$ ,  $i = 1, \dots, n$ , and

$$\Sigma_{\text{contact}}(E) = -\frac{\hbar^2}{2m_x^*} \frac{d^2}{dx^2} e^{ik_l x} \quad (60)$$

where  $k_l$  can be solved from

$$E = E_{l,\text{contact}} + \frac{\hbar^2}{2m_x^*} \frac{d^2}{dx^2} (1 - \cos k_l x) \quad (61)$$

$E_{l,\text{contact}}$  is the eigen-energy determined by the lead (contact).

34/48

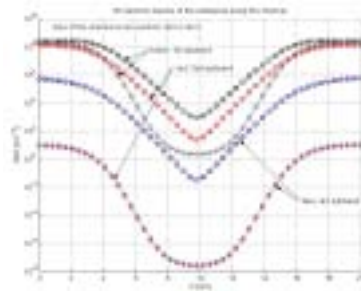


- The density matrix at energy  $E$  is

$$\rho(E) = \frac{1}{\pi} \frac{d}{dx} [F(\mu_s - E)A_S + F(\mu_d - E)A_D] \quad (62)$$

$$A_S = G[i(\Sigma_s - \Sigma_s^+)]G^+, \quad A_D = G[i(\Sigma_d - \Sigma_d^+)]G^+ \quad (63)$$

- 2D electron density for each subband



35/48



- 3D electron density on the cross-section and along the channel.

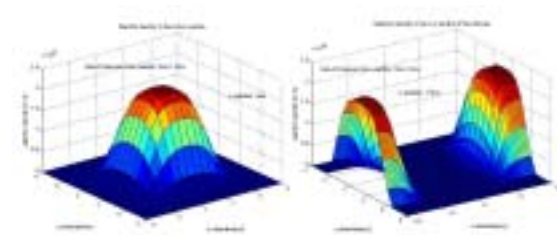
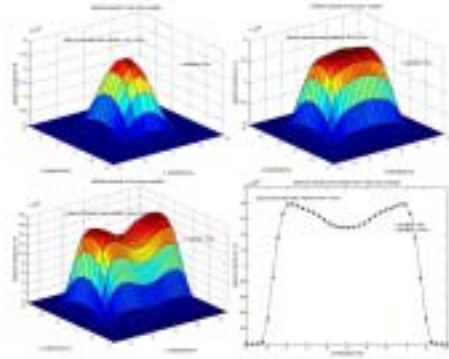


Figure 7: Cross-section: 3 nm × 3 nm

36/48



– Size effect



37/48



–  $I$ - $V$  characteristics

$$I(E) = \frac{2q}{h} [F(\mu_s - E) - F(\mu_d - E)] \text{Tr}[\Gamma_s A_D] = \frac{2q}{h} [F(\mu_s - E) - F(\mu_d - E)] \text{Tr}[\Gamma_d A_S] \quad (64)$$

Where  $\Gamma_s = i[\Sigma_s - \Sigma_s^+]$  and  $\Gamma_d = i[\Sigma_d - \Sigma_d^+]$ .

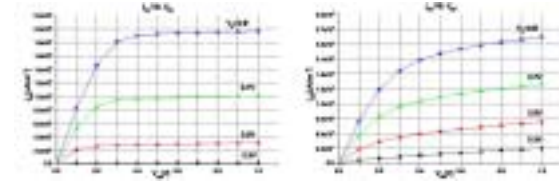


Figure 8:  $L_{ch} = 10, 5$  nm, cross-section:  $3 \text{ nm} \times 3 \text{ nm}$ , and  $t_{ox} = 1$  nm

38/48



## Ballistic MOS Model (BMM) with 2D QM Corrections

Features:

- Ballistic carrier transport along the channel

$$\frac{I_D}{W} = Q(0) \frac{1-r}{1+r} \left[ v_T \frac{\mathcal{F}_{1/2}(\eta)}{\mathcal{F}_0(\eta)} \right] \frac{1 - \frac{\mathcal{F}_{1/2}(\eta - U_D)}{\mathcal{F}_{1/2}(\eta)}}{1 + \frac{1-r}{1+r} \frac{\mathcal{F}_0(\eta - U_D)}{\mathcal{F}_0(\eta)}} \quad (65)$$

where  $v_T$  is the thermal velocity,  $U_D = V_{DS}/V_T$ ,  $\eta = (E_{FS} - E_{\text{max}})/k_B T$ , and back scattering coefficient

$$r = \frac{l}{l + \lambda}, \quad l = L \left( V_T \frac{\beta}{V_{DS}} \right)^\alpha, \quad \lambda = V_T \frac{2\mu}{v_T} \frac{\mathcal{F}_0^2(\eta)}{\mathcal{F}_{-1}(\eta) \mathcal{F}_{1/2}(\eta)}$$

- QM corrected threshold voltage

$$Q(0) = C_{ox} V_{g,\text{eff}} \quad (66)$$

39/48



where  $C_{ox} = \epsilon_{ox}/t_{ox}$  is the gate-oxide capacitance per unit surface area and  $V_{g,\text{eff}}$  is the effective gate voltage,

$$V_{g,\text{eff}} = \frac{2sV_T \ln \left[ 1 + \exp \left( \frac{V_{od}}{2sV_T} \right) \right]}{1 + 2sC_{ox} \sqrt{\frac{2\psi_s}{q\epsilon_0\epsilon_{si}N_{\text{sub}}}} \exp \left[ \frac{V_{od} - 2(V_{GS} - V_{th} - V_{\text{off}})}{2sV_T} \right]} \quad (67)$$

where  $V_{od} = V_{GS} - V_{FB} - \phi_s - Q_{\text{dep}}/C_{ox}$ ,  $s$  swing factor, and  $V_{\text{off}}$  a parameter. The key of the modeling is to find right expression for the threshold voltage

$$V_{th} = V_{th,\text{cl}} + \Delta V_{1D,\text{qum}} + \Delta V_{\text{pg,qum}} + \Delta V_{2D,\text{qum}} \quad (68)$$

According to Natori,

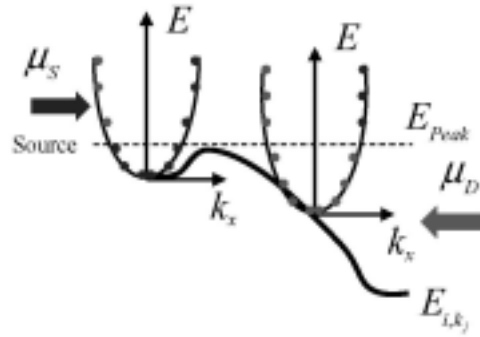
$$Q(0) \approx 2.5 \frac{qkT}{2\pi\hbar^2} \sqrt{m_l m_l} [\ln(1 + e^\eta) + \ln(1 + e^{\eta - U_D})] \quad (69)$$

from which one can find  $\eta$ , given bias.

40/48



Band diagram along the channel



41/48

- 1D-QM correction

$$\Delta V_{1D,qm} = 1 + \frac{1}{2C_{ox}} \sqrt{\frac{2q\epsilon_0\epsilon_{si}N_{sub}}{a_1 + b_1\bar{N}_{sub} + c_1\bar{N}_{sub}^2}} \quad (70)$$

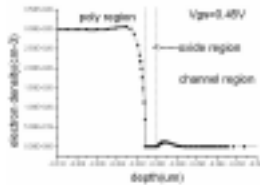
$\bar{N}_{sub} = N_{sub}/10^{18}$ , fitting parameters  $a_1 = 1.02411$ ,  $b_1 = 0.04606$ , and  $c_1 = -0.00206$ .

42/48

- QM in poly gate

$$\Delta V_{pg,qm} = a_p + b_p\bar{N}_{sub} = c_p\bar{N}_{sub} \quad (71)$$

$a_p = 0.01967$ ,  $b_p = 0.01133$ , and  $c_p = \frac{1}{3} \times 10^{-3}$



43/48

- 2D Corrections

The solution to the 3D Schrödinger equation using the separation of variables as follows.

$$\Psi(x, y, z) = \underbrace{\frac{A}{\sqrt{p(x)}} \exp\left(\frac{i}{\hbar} \int^x p(\xi) d\xi\right)}_{X(x)} \cdot \underbrace{\sqrt{\frac{2}{W}} \sin\left(\frac{n_y \pi}{W} y\right)}_{Y(y)} \cdot \underbrace{\varphi_{n_z}(z)}_{Z(z)} \quad (72)$$

With WKB theory,

$$p(x) = \sqrt{2m_x[E - U(x, y, z)]} \quad (73)$$

$$\frac{i}{\hbar} \int_a^b \sqrt{2m_x[E_d - U(x)]} dx = -4 \quad (74)$$

for  $e^{-4} = 1.83\%$  can be considered as negligibly small. The correction to the threshold voltage due to 2D QM effects can

44/48

be expressed as

$$\Delta V_{2D-QM} = \frac{E_d - E_{\text{peak}}}{q} \left( 1 + \frac{1}{2C_{\text{ox}}} \sqrt{\frac{\epsilon_0 \epsilon_{\text{Si}} q^2 N_{\text{sub}}}{k_B T \ln(N_{\text{sub}}/n_0)}} \right) \quad (75)$$

The results by applying the 2D QM correction to the simulation of transfer characteristics.

Analytical approach: approximate  $E_{n_z}(x)$  with a parabola.

$$E_{n_z}(x) \approx E_{\text{peak}} - \sigma(x - x_{\text{max}})^2 \quad (76)$$

And obtain

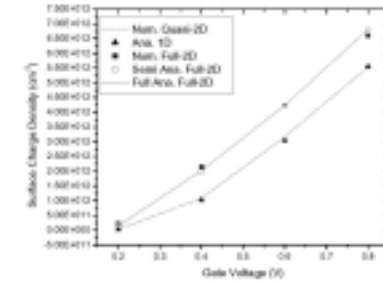
$$E_d - E_{\text{peak}} = \frac{8\hbar}{\pi} \sqrt{\frac{\sigma}{2m_x}} \quad (77)$$

The fitting parameter  $\sigma$  is less sensitive to  $t_{\text{ox}}$  and  $N_{\text{sub}}$ , but strongly depends on the channel length  $L$ . An empirical formula is

$$\sigma = 4.73 \times 10^{-3} e^{-L/16} \quad (78)$$



45/48



where  $L$  in units nm.



46/48

## Simulation Examples using BMM

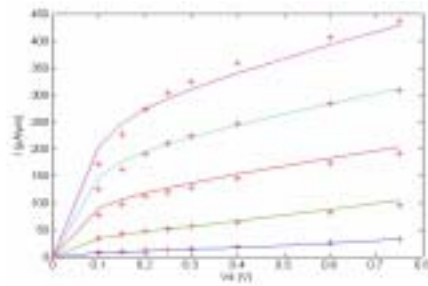


Figure 9: Modeling of 14 nm MOSFET (A. Hokazono *et al.*, 2002) with BMM,  $V_{gs} = 0.25 - 0.65$  V of step 0.1 V.



47/48

## Conclusions

- QM effects become first-order ones in nano-scale MOS-FETs
- Robust macroscopic model(s) now exists for device simulation
- Wavefunction based approach may find broad application in nanoelectronic devices
- The built-in of QM effects in compact model likely will take the similar path to the “surface potential” approach.



48/48